

Design and Development of Laminated Aluminum Glass Fiber Drive Shaft for Light Duty Vehicles

M.Arun, K.Somasundara Vinoth

Abstract—A drive shaft, also known as a propeller shaft or cardan shaft, it is a mechanical part that transmits the torque generated by a vehicle's engine into usable motive force to propel the vehicle. Now a day's two piece steel shaft are mostly used as a drive shaft. The two-piece steel drive shaft consists of three universal joints, a center supporting bearing and a bracket, which increases the total weight of an automotive vehicle and decreases fuel efficiency. This work deals with the replacement of conventional two piece steel drive shafts with a one piece Hybrid Aluminum E glass/epoxy composite drive shaft for an automotive application. The basic requirements considered here are torsional strength, torsional buckling and bending natural frequency. A hybrid of Aluminum and E-glass/epoxy as in which the aluminum has a role to transmit the required torque, while the E-Glass epoxy composite increases the bending natural frequency. An experimental study was carried out to study the static torsion capability. Four cases were studied using aluminum tube wounded by different layers of composite materials. Results obtained from this study show that increasing the number of layers would enhance the maximum static torsion approximately 66% for $[+45/-45]_3$ laminates higher than the pure aluminum and mass reduction of 42% compared with of steel drive shaft. A one-piece hybrid composite full drive shaft is optimally analyzed using Finite Element Analysis Software and simulation results were compared with the existing steel drive shaft.

Index Terms— One-piece hybrid aluminum/composite drive shaft, Static torque capability, buckling torque capability, bending natural frequency, E-glass fiber, Static Analysis, Modal Analysis, ANSYS.

I. INTRODUCTION

An automotive drive shaft transmits power from the engine to the differential gear of a rear wheel drive vehicle as shown in Fig.1 [1]. In the past many researchers have investigated the use of hybrid drive shafts. For automotive application, the first composite drive shaft was developed by the Spicer U-Joint division of Dana Corporation for Ford econoline van models in 1985. The General Motors pickup trucks which adopted the Spicer product enjoyed a demand three times that of project sales in its first year, i.e. in 1988, [1,3]. The two main functional requirements for power transmission rotating shafts such as drive shafts of machinery and automotive propeller shafts are the transmission of static and dynamic torsional loads and the high fundamental bending natural frequency to avoid whirling vibration at a high rotational speed.

Long shafts made of conventional material such as aluminum and steel cannot satisfy easily these two functional requirements simultaneously because they have lower specific stiffness, which limits the magnitude of fundamental bending natural frequency [2]. The static torque capability of the drive shaft for passenger cars should be larger than 2700Nm and the fundamental bending natural frequency should be higher than 9200rpm to avoid whirling vibration [1]. Since the fundamental bending natural frequency of one-piece drive shafts made of steel or aluminum is normally lower than 5700rpm when the length of the drive shaft is around 1.2m [1], the steel drive shaft is usually manufactured in two pieces to increase the fundamental bending natural frequency because the bending natural frequency of a shaft is inversely proportional to the square of beam length and proportional to the square root of specific modulus. The two-piece steel drive shaft consists of three universal joints, a center supporting bearing and a bracket, which increases the total weight of automotive vehicle and decreases fuel efficiency. Since high modulus carbon fiber epoxy composite materials have more than 10 times specific stiffness (E/ρ) of steel or aluminum materials, it is possible to manufacture composite drive shafts in one piece without whirling vibration over 9200rpm [1].

Hybrid shafts composed of aluminum and glass fibers can withstand more torque. The composite drive shaft has many benefits such as reduced weight, less noise and vibration [1]. Hybrid shafts composed of aluminum and glass fibers can withstand more torque. However, because of the high material cost of carbon fiber epoxy composite, rather inexpensive aluminum materials and glass fiber may be used combined partly with composite materials to make a hybrid type aluminum/composite drive shaft, in which the aluminum has a role to transmit the required torque while the glass fiber epoxy composite increases the bending natural frequency. Furthermore a one-piece propeller shaft for rear wheel drive automobiles was designed and manufactured with carbon fiber epoxy composites based on the specifications, such as static torque transmission capability, torsional buckling capability and fundamental natural bending frequency. The composite propeller shaft had about 40% weight saving compared with a two-piece steel propeller shaft. [7]. In another study, genetic algorithm (GA) was used to minimize the weight of one-piece propeller shaft for rear wheel drive automobiles [8], which is subjected to constraints such as torque transmission, torsional buckling capacities and fundamental of natural frequency.

Manuscript received May, 2013.

Arun M, Department of Production Engineering, PSG College of Technology, Coimbatore-641004, India.

K.Somasundara Vinoth, Assistant Professor and Research Scholar, Department of Production Engineering, PSG College of Technology, Coimbatore-641004, India.

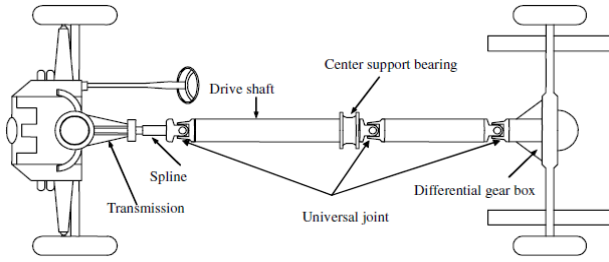


Fig 1 .Schematic diagram of the conventional two - piece steel drive shaft for rear wheel drive vehicle

II. SPECIFICATION OF THE PROBLEM

The torque transmission capability of the drive shaft for passenger cars, small trucks, and vans should be larger than 3500 Nm (Tmax) and fundamental natural bending frequency of the drive shaft should be higher than 6500 rpm (Nmax) to avoid whirling vibration. The drive shaft outer diameter do should not exceed 100 mm due to space limitations. Here outer diameter of the shaft is taken as 90.5 mm and length L of the drive shaft considered here is 1320 mm. The drive shaft of transmission system was designed optimally to the specified design requirements

III. DESIGN OF STEEL DRIVE SHAFT

Presently, steel (SM45C) is used for making automotive drive shafts. The material properties of the steel (SM45C) are given in Table 1 [10]. The steel drive shaft should satisfy three design specifications such as torque transmission capability, buckling torque capability and bending natural frequency.

A . Torque transmission capacity of the steel drive shaft

Torque transmission capacity T of a steel drive shaft is given by:

$$T = S_s \frac{\pi(d_o^4 - d_i^4)}{16d_o} \tag{1}$$

where S_s is the shear strength, d_o and d_i represent outside and inside diameter of the steel shaft.

Table 1.Mechanical properties of steel

Mechanical properties	Symbol	Steel
Young's modulus (GPa)	E	207.0
Shear modulus (GPa)	G	80.0
Poisson's ratio	v	0.3
Density (Kg/m ³)	ρ	7600
Yield strength (MPa)	S _y	370
Shear strength (MPa)	S _s	370

B. Torsional Buckling Capacity of steel drive shaft

$\frac{1}{\sqrt{1 - \nu^2}} \frac{L^2 t}{(2r)^3} > 5.5$, it is called as long shaft otherwise it is called as short & medium shaft [11]. For a long shaft, the critical stress τ_{cr} is given by:

$$\tau_{cr} = \frac{E}{3\sqrt{2}(1 - \nu^2)^{3/4}} (t/r)^{3/2} \tag{2}$$

where E, and ν represent steel properties. L, t and r are the length, thickness and mean radius of the shaft respectively. The relation between the torsional buckling capacity T_{cr} and critical stress is given by:

$$T_{cr} = \tau_{cr} 2\pi r^2 t \tag{3}$$

C. Lateral Vibration of steel drive shaft

The shaft is considered as simply supported beam undergoing transverse vibration or can be idealized as a pinned-pinned beam. Natural frequency f_{nt} is calculated using Timoshenko beam theory [12]. It considers both transverse shear deformation as well as rotary inertia effects. Natural frequency based on the Timoshenko beam theory is given by:

$$f_{nt} = K_s \frac{30\pi p^2}{L^2} \sqrt{\frac{Er^2}{2\rho}} \tag{4}$$

where f_{nt} is the natural frequency and p is the first natural frequency. E and ρ are the material properties of the steel shaft, and K_s is given by:

$$\frac{1}{K_s^2} = 1 + \frac{p^2 \pi^2 r^2}{2L^2} \left[1 + \frac{f_s E}{G} \right] \tag{5}$$

where G is the rigidity modulus of the steel shafts and f_s = 2 for hollow circular cross-sections.

Critical speed of steel Drive shaft given by:

$$N_{crit} = 60f_{nt} \tag{6}$$

III. DESIGN OF THE ALUMINUM/COMPOSITE DRIVE SHAFT

The aluminum/composite drive shaft should satisfy three design specifications such as static torque capability, buckling torque capability and bending natural frequency. The major role of the aluminum tube is to sustain an applied torque while the role of the glass fiber epoxy composite is to increase bending natural frequency. The aluminum used in this work is AA 6063. Table 2 and 3 mechanical properties of Aluminum (T6-6063) and E Glass/Epoxy respectively.

Table 2.Mechanical properties of Aluminum (T6-6063)

Mechanical Properties	Symbol	Units	Steel
Young's Modulus	E	GPa	72
Shear modulus	G	GPa	27
Poisson Ratio	ν	-	0.33
Density	P	Kg/m ³	2700
Yield Strength	Sy	Mpa	131
Shear Strength	Ss	Mpa	150

A. Selection of cross-section and materials

The following assumptions were made in calculations:

- The shaft rotates at a constant speed about its longitudinal axis;
- The shaft has a uniform, circular cross section;
- The shaft is perfectly balanced, i.e., at every cross section, the mass center coincides with the geometric center;
- All damping and nonlinear effects are excluded;
- The stress-strain relationship for composite material is linear & elastic; hence, Hook's law is applicable for composite materials;
- Since lamina is thin and no out-of-plane loads are applied, it is considered as under the plane stress.

The aluminum used to make hybrid drive shaft can be solid circular or hollow circular. In this work hollow circular cross-section was chosen because the hollow circular shafts are stronger in per kg weight than solid circular and the stress distribution in case of solid shaft is zero at the center and maximum at the outer surface while in hollow shaft stress variation is smaller. In solid shafts the material close to the center are not fully utilized.

$E_{11}, E_{22}, G_{12}, \nu_{12}, \nu_{21}, \sigma_1, \sigma_2$ and σ_2 represent lamina properties in longitudinal and transverse directions respectively. ν_f, τ_{12}, ρ and V_f are the Poisons ratio, shear stress and fiber volume fractions.

Table 3 .Mechanical properties of the E-Glass Epoxy

Mechanical Properties	Symbol	Units	E-Glass Epoxy
Longitudinal Young's Modulus	E_{11}	Gpa	52.36
Transverse Young's Modulus	E_{22}	Gpa	8.02
Major Poisson Ratio	ν_{12}		0.24
Inplane Shear Modulus	G_{12}	Gpa	3.097
Ultimate Longitudinal Tensile Strength	$(\sigma_1^t)_{wt}$	Mpa	954.8
Ultimate Longitudinal Compressive Strength	$(\sigma_1^c)_{wt}$	Mpa	69.2
Transverse Tensile Strength	$(\sigma_2^t)_{wt}$	Mpa	27.29
Ultimate Transverse Compressive Strength	$(\sigma_2^c)_{wt}$	Mpa	38.66
Inplane shear strength	$(\tau_{12})_{wt}$	Mpa	12.72
Density	P	Kg/m ³	1980

B.Design procedure for composite

a) Stress-Strain Relationship for Unidirectional Lamina

The lamina is thin and if no out-of-plane loads are applied, it is considered as the plane stress problem. Hence, it is possible to reduce the 3-D problem into 2-D problem. For unidirectional 2-D lamina, the stress-strain relationship in whereterms of principal material directions is given by:

$$\begin{Bmatrix} \sigma_1 \\ \sigma_2 \\ \tau_{12} \end{Bmatrix} = \begin{bmatrix} Q_{11} & Q_{12} & 0 \\ Q_{12} & Q_{22} & 0 \\ 0 & 0 & Q_{66} \end{bmatrix} \begin{Bmatrix} \varepsilon_1 \\ \varepsilon_2 \\ \gamma_{12} \end{Bmatrix} \quad (7)$$

where σ, τ, γ and ε represent stresses and strains in material directions. The matrix Q is referred to as the reduced stiffness matrix for the layer and its terms are given by:

$$Q_{11} = \frac{E_{11}}{1 - \nu_{12}\nu_{21}}; \quad Q_{12} = \frac{\nu_{12}E_{22}}{1 - \nu_{12}\nu_{21}};$$

$$Q_{22} = \frac{E_{22}}{1 - \nu_{12}\nu_{21}}; \quad Q_{66} = G_{12}.$$

b) Stress strain relation in arbitrary orientation

For an angle-ply lamina, where fibers are oriented at an angle with the positive X-axis (longitudinal axis of shaft), the stress strain relationship is given by:

$$\begin{Bmatrix} \sigma_x \\ \sigma_y \\ \tau_{xy} \end{Bmatrix} = \begin{bmatrix} \bar{Q}_{11} & \bar{Q}_{12} & \bar{Q}_{16} \\ \bar{Q}_{12} & \bar{Q}_{22} & \bar{Q}_{26} \\ \bar{Q}_{16} & \bar{Q}_{26} & \bar{Q}_{66} \end{bmatrix} \begin{Bmatrix} \varepsilon_x \\ \varepsilon_y \\ \gamma_{xy} \end{Bmatrix} \quad (8)$$

where σ and ε represent normal stresses and strains in X, Y and XY dirctions respectively and bar over Q_{ij} matrix denotes transformed reduced stiff nesses.

C. Force and moment resultants

For a symmetric laminate, the B matrix vanishes and the in plane and bending stiffnesses are uncoupled.

$$\begin{Bmatrix} N_x \\ N_y \\ N_{xy} \end{Bmatrix} = \begin{bmatrix} A_{11} & A_{12} & A_{16} \\ A_{12} & A_{22} & A_{26} \\ A_{16} & A_{26} & A_{66} \end{bmatrix} \begin{Bmatrix} \varepsilon_x^o \\ \varepsilon_y^o \\ \gamma_{xy}^o \end{Bmatrix} \quad (9)$$

$$\begin{Bmatrix} M_x \\ M_y \\ M_{xy} \end{Bmatrix} = \begin{bmatrix} D_{11} & D_{12} & D_{16} \\ D_{12} & D_{22} & D_{26} \\ D_{16} & D_{26} & D_{66} \end{bmatrix} \begin{Bmatrix} \kappa_x^o \\ \kappa_y^o \\ \kappa_{xy}^o \end{Bmatrix} \quad (10)$$

where N_x, N_y, N_{xy} and M_x, M_y, M_{xy} in (9), (10) referred as forces and moments per unit width.

$$A_{ij} = \sum_{k=1}^n (\bar{Q}_{ij})_k (h_k - h_{k-1}); \quad (11a)$$

$$B_{ij} = \frac{1}{2} \sum_{k=1}^n (\bar{Q}_{ij})_k (h_k^2 - h_{k-1}^2) \quad (11b)$$

$$D_{ij} = \frac{1}{3} \sum_{k=1}^n (\bar{Q}_{ij})_k (h_k^3 - h_{k-1}^3) \quad (11c)$$

where represent A_{ij}, B_{ij} and D_{ij} are extensional, coupling and bending stiffnesses having $i, j = 1, 2...6$ respectively, h_k is the distance between the neutral fiber to the top of the K^{th} layer. Strains in the reference surface is given by:

$$\begin{Bmatrix} \varepsilon_x^o \\ \varepsilon_y^o \\ \gamma_{xy}^o \end{Bmatrix} = \begin{bmatrix} a_{11} & a_{12} & a_{16} \\ a_{12} & a_{22} & a_{26} \\ a_{16} & a_{26} & a_{66} \end{bmatrix} \begin{Bmatrix} N_x \\ N_y \\ N_{xy} \end{Bmatrix} \quad (12)$$

where

$$\begin{bmatrix} a_{11} & a_{12} & a_{16} \\ a_{12} & a_{22} & a_{26} \\ a_{16} & a_{26} & a_{66} \end{bmatrix} = \begin{bmatrix} A_{11} & A_{12} & A_{16} \\ A_{12} & A_{22} & A_{26} \\ A_{16} & A_{26} & A_{66} \end{bmatrix}^{-1}$$

4.2.4 Elastic constants for the composite shaft

Elastic constants for the composite shaft are given by:

$$E_x = \frac{1}{t} \left[A_{11} - \frac{A_{12}^2}{A_{22}} \right]; \quad E_y = \frac{1}{t} \left[A_{22} - \frac{A_{12}^2}{A_{11}} \right],$$

where E_x and E_y are the Young's modulus of the shaft in axial and hoop direction:

$$G_{xy} = \frac{A_{66}}{t}; \quad \nu_{xy} = \frac{A_{12}}{A_{11}},$$

When a shaft is subjected to torque T, the resultant forces N_x, N_y, N_{xy} in the laminate by considering the effect of centrifugal forces are:

$$N_x = 0; \quad N_y = 2\rho t r^2 \omega^2; \quad N_{xy} = \frac{T}{2\pi r^2} \quad (13)$$

where ρ is the density, t is the thickness, r mean radius and ω

is the angular velocity of the composite shaft knowing the stresses in each ply, the failure of the laminate is determined using the first ply failure criteria. That is, the laminate is assumed to fail when the first ply fails. Here maximum stress theory is used to find the torque transmitting capacity.

D. Torque transmitted by the hybrid drive shaft

The torque transmitted by the hybrid drive shaft, T is the sum of the torque transmitted by the aluminum tube, T_{al} and that by the composite layer, T_{co} [11, 13]:

$$T = T_{al} + T_{co} \tag{14}$$

Considering geometric compatibility and material properties of each material, the torque transmitted by the aluminum tube is calculated as follows:

$$T_{al} = \frac{G_{al} \cdot J_{al}}{G_{al} \cdot J_{al} + G_{com} \cdot J_{com}} T \tag{15}$$

where G is shear modulus, J is the polar moment of inertia, and subscripts al and co represent the aluminum tube and the composite layer, respectively. The shear modulus G_{al} and the polar moment of inertia of the aluminum tube J_{al} are much larger than those of the composite layer because only thin layer of unidirectional composite can increase sufficiently the natural frequency of the hybrid drive shaft. Therefore, the torque transmitted by the aluminum tube only is almost same as the torque transmitted by the hybrid aluminum/composite shaft. From now on, the static and buckling torque capabilities of the aluminum/composite shaft will be calculated neglecting the composite layer as follows [11]:

$$T_{static} = 2\pi \cdot r_{ave}^2 \cdot t_{al} \cdot S_{S,al} \tag{16}$$

$$T_{buckling} = \frac{\pi\sqrt{2} \cdot E_{al}}{3(1 - \nu_{al}^2)^{0.75}} \sqrt{(r_{ave} \cdot t_{al}^5)} \tag{17}$$

where T_{static} and $T_{buckling}$ are the static and buckling torque capabilities of the hybrid aluminum/composite shaft respectively, and r_{ave} is the average radius of the aluminum tube, t_{al} is the thickness of the aluminum tube, $S_{S,al}$ is the shear strength of the aluminum, E_{al} is the elastic modulus of aluminum, and ν_{al} is the poisson's ratio of aluminum. The static and buckling torque capabilities of the aluminum/composite shaft are shown in Fig. 2 and Fig. 3 with respect to the outer diameter ($2 \cdot r_{ave} + t_{al}$) and thickness (t_{al}) of the aluminum tube. Since the outer diameter of the drive shaft is normally limited to 100 mm for passenger cars, the outer diameter and thickness of the aluminum tube were determined to be 90 mm and 2 mm, respectively.

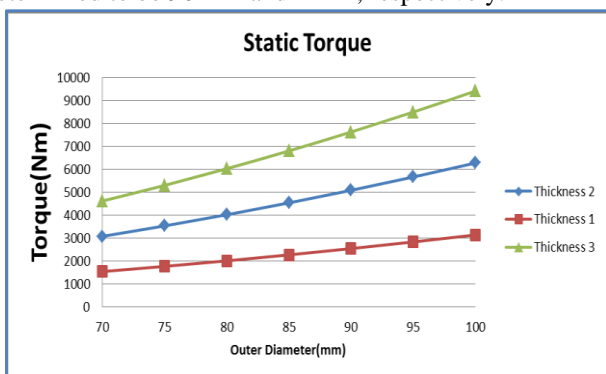


Fig 2 Static Torque capability of the aluminum tube with respect to the outer diameter and thickness t_{al} of the aluminum tube calculated from Eqs. (16) (Design torque ≥ 3500 Nm).

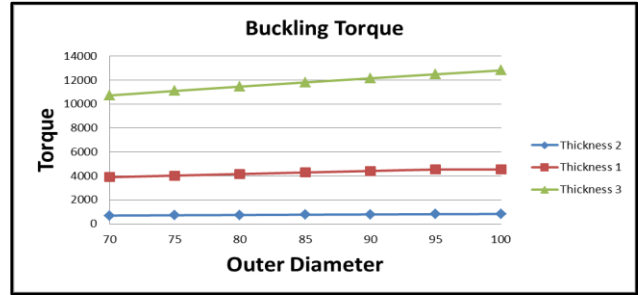


Fig 3 Buckling Torque capability of the aluminum tube with respect to the outer diameter and thickness t_{al} of the aluminum tube calculated from Eqs. (17) (Design torque ≥ 3500 Nm)

E. Fundamental bending natural frequency of drive shafts

The fundamental bending natural frequency of drive shafts f_n was calculated by the following equation with the simply supported boundary condition on the both ends [14].

$$f_n = \frac{9.869}{L^2} \sqrt{\frac{E_{al}I_{al} + E_{co}I_{co}}{\rho_{al} + \rho_{co}}} \tag{17}$$

where E is the elastic modulus in the axial direction of drive shaft, I is the sectional moment of inertia, ρ is the mass per unit length, and L is the length of the drive shaft.

E. Lay-up selection

It is well-known that the shear modulus of many fiber-reinforced composites is lower than that for steel. Thus for an equivalent torsional stiffness, a fiber-reinforced composite tube must have either a larger diameter or a greater thickness than a steel tube [15]. Among the various laminate configurations, $[\pm 45]_s$ laminates possess the highest shear modulus and are the primary laminate type used in purely torsional applications [16]. Therefore, the lay-up selected consists of $[\pm 45^\circ]$ glass fiber layers.

IV. EXPERIMENTAL WORK

The prospective results of experimental work are aimed to irrefutably investigate the torsional strength of the composite drive shaft. The behavior of composite tube under fiber orientation angle $[\pm 45]$ with different layers should be investigated. Glass mat fabrics are used with epoxy wounded with aluminum to manually fabricate composite tubes with dimensions scaled down from the designed drive shaft.

A. Geometry and Materials

The aluminum tube (AA6063) used for this investigation. The size of the torsion showed in table 4. The torsion specimen dimension has the outer diameter and the thickness (22 and 3) mm, respectively. The fiber used for the hybrid aluminum/composite tube is of glass fibers type. The epoxy resin and hardener types used in this study were of MW 215 TA and MW 215 TB respectively, Table 6 shows the physical properties of epoxy and hardener. E-glass fibers were used in this work.

Table 6 Physical Properties of Epoxy and Hardener

Item	Unit	WM-215TA	WM-215TB
Appearance		White Viscous Liquid	Colorless Liquid
Viscosity	Cps@ 30C	5500	30
Mixing ration	-	100	25

B. Fabrication of a Hybrid Aluminum/Composite Drive Shaft torsion

Six layers glass/epoxy were wrapped around aluminum tubes of length equal to 410 mm and outside diameter equal to 22 mm for torsion specimen. Resin system was prepared by mixing epoxy, and hardener with the volume fraction ratio of 4:1. The torsion specimen images are shown below in figure 4



a) Aluminum tube



c) Aluminum with 4 layers



d) Aluminum with 6 Layers

Fig 4 Torsion specimen images of Hybrid Drive Shaft



Fig 5 Lathe machine used to cut the specimen ends to its final dimensions

The specimens were fabricated in such a way that the stress level in central gauge section must be greater than in all other

structure points. This will be done by paying a particular attention to end effect problem which is a point of concentration stresses at the aluminum/composite drive shaft. The aim of the reinforced ends is to avoid failure within the end regions and eliminate or, at least, minimize concentration of stresses. This additional stresses may cause end failure for loads smaller than those tolerated by the same drive shaft with uniform stress distribution. The selection of specimen tube size for static torsion test is dictated by the capacity of the machine test [9]. After the solidification and the curing time is done, the lathe machine would be used to cut the specimen ends to its final dimensions. The lathe machine used is shown in fig.5

C. Static Torque Test of the Hybrid Shaft:

Torsion test machine was used to perform the test. The testing machine with a specimen mounted on it, is shown in Fig. 6. The torque was applied manually by a handle at a geared head. This torque is reacted by a transducer and displayed digitally. The angle of twist was measured over a specified gauge length. Four cases with different number of layers used for the hybrid aluminum glass fiber shaft as shown in Table 5. The maximum static torsion was obtained after the failure of the specimens and torque- angle of twist relations were obtained for different cases.

Table 5 Torsion specimen dimensions of Hybrid shaft

Specimen	Outer Diameter of Aluminum(mm)	Inner Diameter of Aluminum(mm)	Length of the specimen (mm)	Number of layers Of composite	Thickness of the composite	Fiber orientation
Specimen - I	22	19	410	-	-	
Specimen - II	22	19	410	2	0.25	±45
Specimen - III	22	19	410	4	0.5	±45
Specimen - IV	22	19	410	6	0.75	±45

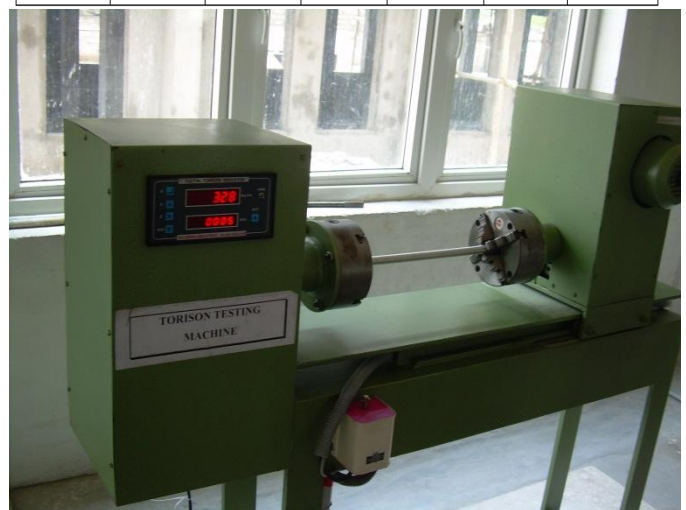


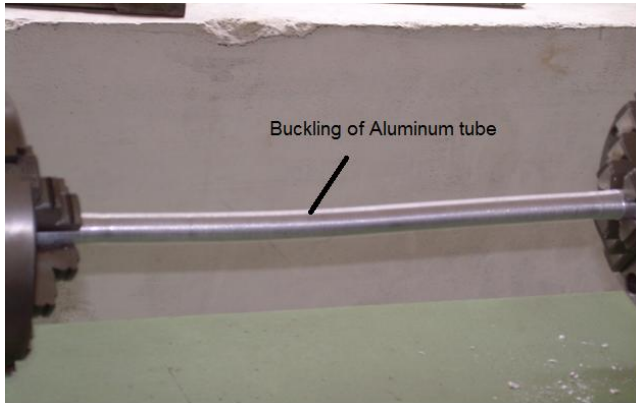
Fig 6 Torsion testing machine holding hybrid drive shaft specimen



Fig 7 Digital Torsion Indicator image on Torsion Testing machine

D. Failure modes on hybrid drive shaft specimen during torsion testing

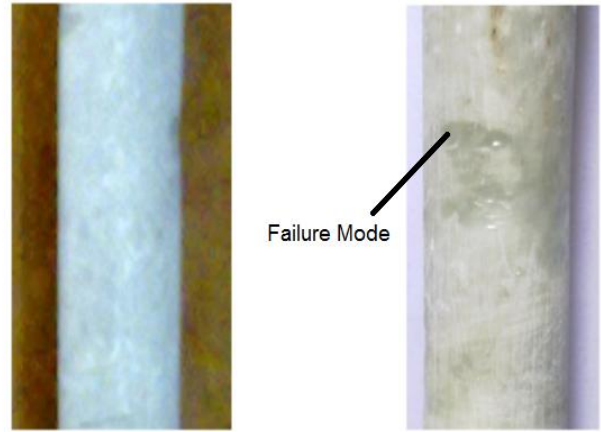
Here ductile failure occurred on torsion specimen due to the shear stresses applied. The ductile failure produces the fracture surface along the plane of the maximum shear stress and more frequently normal to the longitudinal axis of torsion specimen of drive shaft. The torsional failure of shaft occurred when the shearing stresses attain the yield stress of the shaft. The greatest shearing stresses in a hollow shaft occur in a cross-section and along the length of the shaft.



a) Buckling of aluminum tube during torsion testing



b) Delamination of composite layers from the aluminum tube



Specimen before torsion testing

Specimen after torsion testing

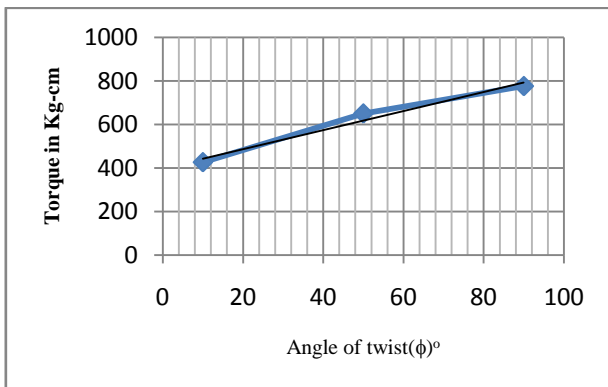
Fig 8 Failure mode of Drive shaft torsion specimen

Hybrid shaft specimen failed by breaking off over a normal cross-section. It was found that the aluminum tube initially yielded first, followed by the crack propagation in composite shaft along the fiber direction. This eventually caused the delamination of composite layers from the aluminum tube, and then the white regions appear in composite layers and finally the fiber breakage and the catastrophic failure took place as shown in fig 8.

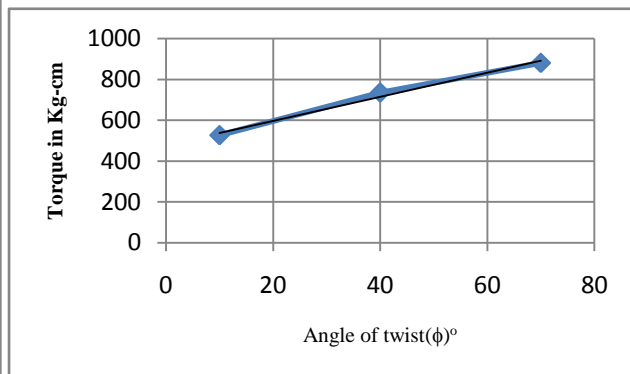
V. RESULTS AND DISCUSSION

In this section, both finite element analysis and experimental results were presented. FEA used to validate date the experimental results and used to compare design of full-scale drive shaft with the existing steel drive shaft. Finite element analysis utilized to study the mechanical behavior of composite drive shaft. The experiments oriented to study the torsional stiffness with its relation to the type of material, fibers orientation angle and number of layers increased. Studying failure modes were another intension of experimental work.

A. Results of torsion testing



a) Aluminum



b) Aluminum with 2 layers

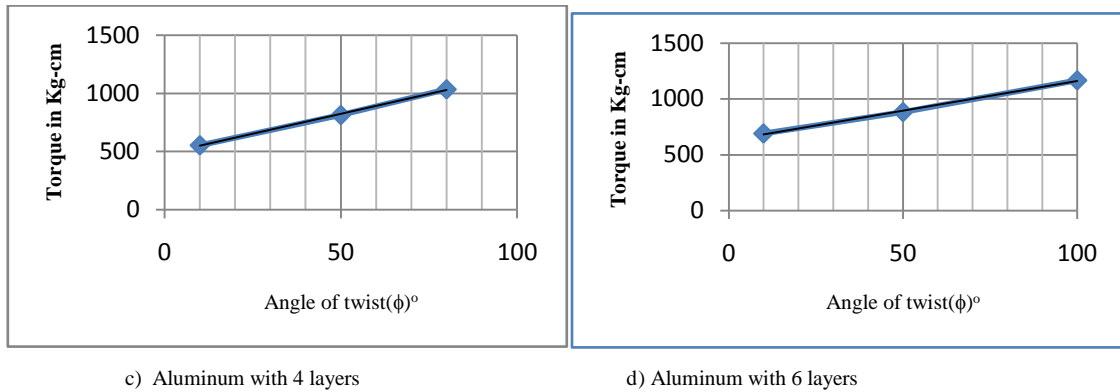


Fig 9 Angle of twist (Φ)^o vs Torque in Kg-cm for Aluminum with six layers

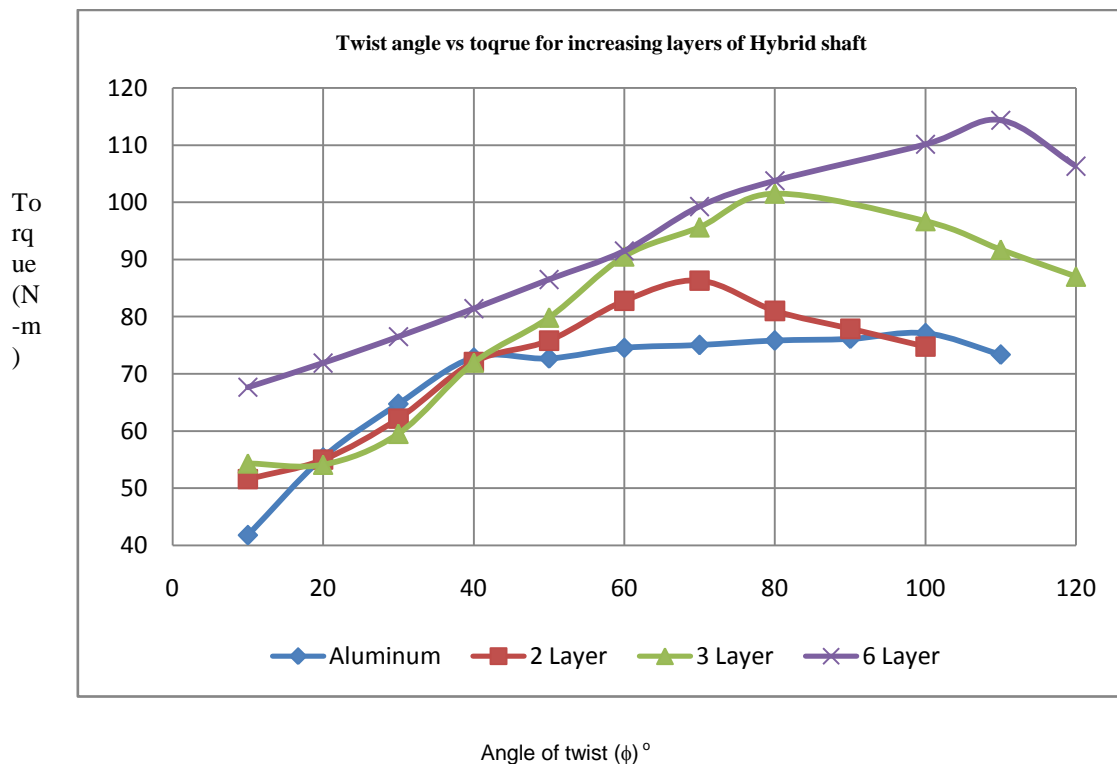


Fig 10 Relationship between Angle of twist(Φ)^o vs Torque (N-m) for increasing layers of composite over aluminum tube

torque for Aluminum and Aluminum with two layers $[\pm 45]_2$ and six layers $[\pm 45]_3$ respectively. Angle of twist vs torque (Kg-cm) values for each cases plotted in fig 12. The behavior of hybrid shaft till 40° angle of twist is the same all layers, at this region the Aluminum tubes still in elastic limit and a linear relation between the applied torque and angle of twist, after this point the aluminum tube material enter in non-elastic region. The static torque capability of the aluminum will be calculated follows as per formula 16 discussed in section 4.3

$$T_{static} = 2\pi \cdot r_{ave}^2 \cdot t_{al} \cdot S_{s,al}$$

From this formula the static torque is 41.03 N.m for aluminum tube. After this limit the static torque of 45° higher than the glass fiber till the point of failure. Failure mode of drive shaft specimens during torsion testing already discussed in section 4.3. The maximum torque obtained in torsion testing before failure for aluminum with six layer $[\pm 45]_3$ is 114 N-m which is 66% higher than the aluminum

tube. Fig 10 shows the relationship between Angle of twist vs Torque (N-m) for increasing layers of composite over aluminum tube. Also it can be seen from Fig. 11 the shear stress values indicate that by increasing the number of layers can enhance the static torsion capacity for the hybrid aluminum glass fiber composite shaft.

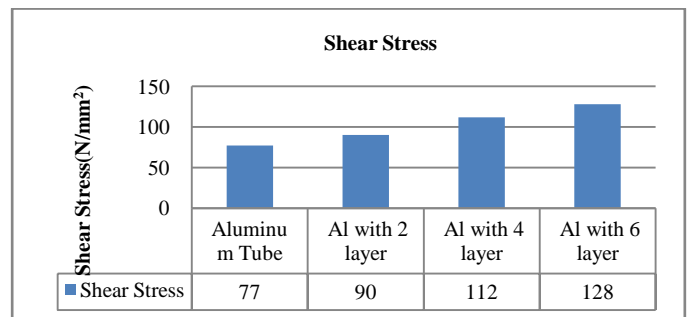
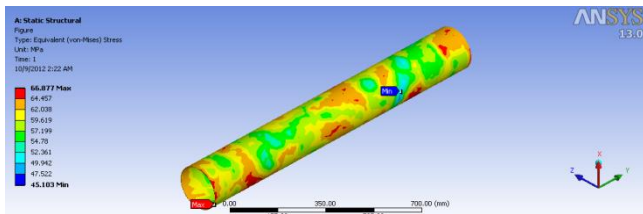


Fig 11 Comparison of shear stress values of Aluminum with increasing layers of composite over aluminum tube

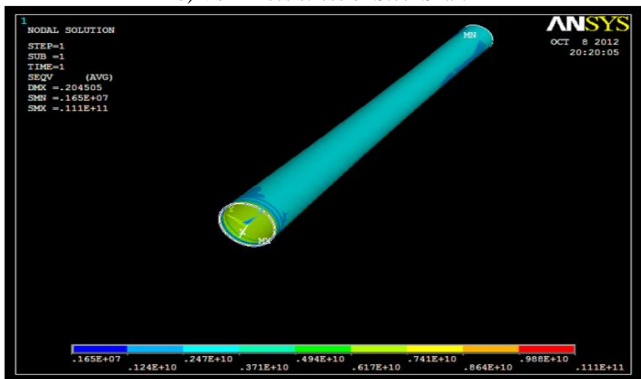
B. Validation of finite element analysis

The devising of a mathematical model in finite element analysis requires a reliable input data to predict the physical behavior of this model. The data about geometry, element, loads, boundary conditions and material properties is the source of uncertainty in the FEA results validity. In this study, analysis for full-scale Hybrid drive shaft was carried out and it is compared with existing steel drive shaft for the same full scale dimensions. The software used to perform FEA analysis is ANSYS. Type of analysis performed for full scale drive shaft is Static, Modal and Harmonic analysis. The shaft is fixed at both ends and is subjected to torque at the end for static analysis and middle for the modal analysis. Here the design torque taken is 3500 Nm and critical speed of shaft is taken as 6500 rpm (108 Hz) to avoid whirling vibration. The element used for analysis is SHELL 181. SHELL181 is suitable for analyzing thin to moderately-thick shell structures. It is a four-node element with six degrees of freedom at each node: translations in the x, y, and z directions, and rotations about the x, y, and z-axes. (If the membrane option is used, the element has translational degrees of freedom only). SHELL181 may be used for layered applications for modeling composite shells or sandwich construction. The accuracy in modeling composite shells is governed by the first-order shear-deformation theory (usually referred to as Mindlin-Reissner shell theory).

a) Results of static Analysis

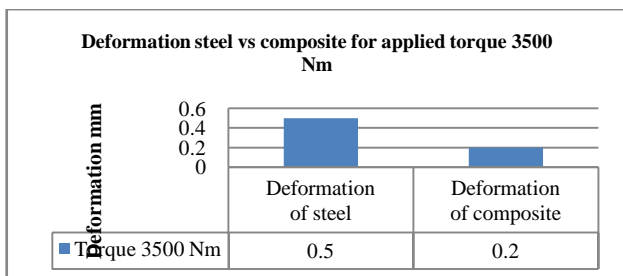


b) Von Mises stress of Steel Shaft

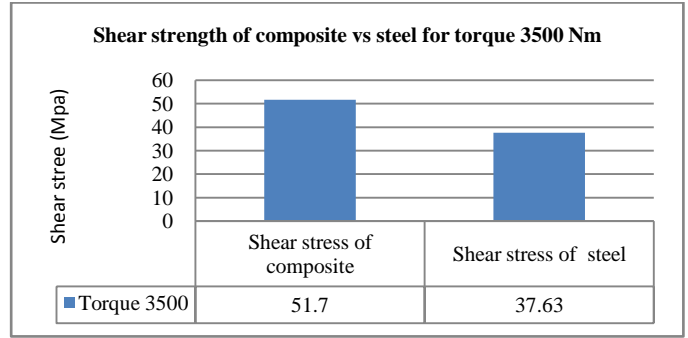


a) Von Mises stress of Hybrid Shaft

Fig 12 Static Analysis of Hybrid shaft and steel shaft



a) Deformation of steel vs hybrid shaft for Design torque ≥ 3500 Nm.



b) Shear stress of steel vs hybrid shaft for Design torque ≥ 3500 Nm.

Fig 13 Results of static analysis

In the static analysis for the applied torque 3500 Nm, the Design Von Mises Stress obtained for hybrid drive shaft is 6 times the allowable stress and higher than that of steel drive shaft. Shear stress obtained for hybrid shaft is 37% higher than steel drive shaft and for the same torque applied the total deformation of the hybrid shaft is 60% less than steel drive shaft. So the newly developed Hybrid Aluminum E Glass Epoxy Drive shaft will satisfy the torsional capabilities requirements and safe as steel drive shaft.

b) Results of modal Analysis

The drive shaft rotates with maximum speed so the design should include a critical frequency. If the shaft rotates at its natural frequency, it can be severely vibrated or even collapsed. The modal analysis is performed to find the natural frequencies in lateral directions. The mode shapes for all material combinations are obtained to their corresponding critical speeds. A number of fundamental modes, which all are critical frequencies, are obtained. If the shaft's frequencies correspond to these ones, it may be collapsed.

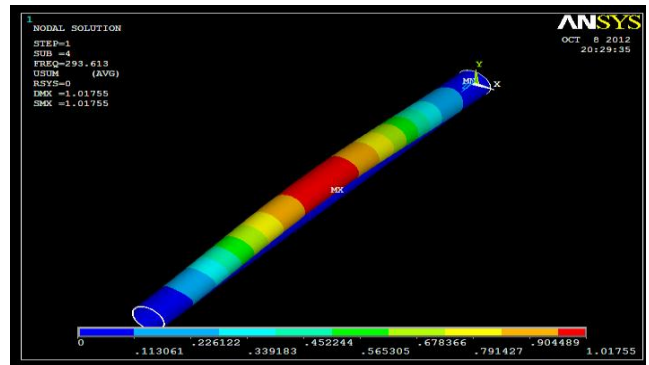


Fig Deformation of a Hybrid drive shaft for 4th Mode (293.613 Hz (17616.78 rpm))

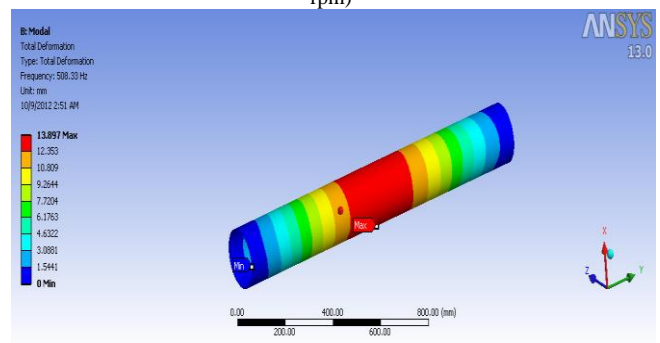


Fig 14 Deformation of a steel drive shaft for first mode 508.33 Hz (30499 rpm)

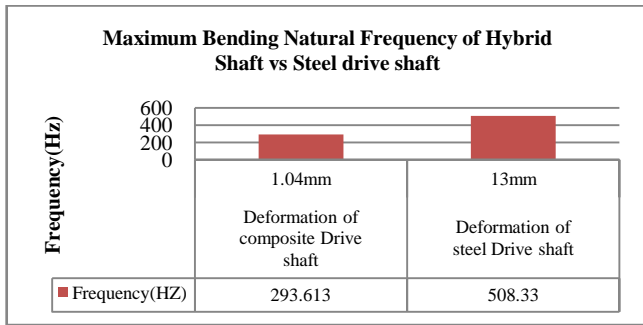


Fig 15 Maximum bending natural frequency of steel vs. composite

The bending natural frequency is the frequency of the shaft in which it becomes unstable. Bending natural frequency for steel drive shaft is one and half times higher than the hybrid composite drive shaft. But the requirement is only 108 Hz (6500rpm) as per design specification in which the hybrid shaft can withstand 293 Hz (17616 rpm). So the Hybrid Drive Shaft satisfies the vibrational requirements of the drive shaft.

VII. CONCLUSION

In this work, a one-piece hybrid aluminum/composite drive shaft for a rear wheel drive automobile was designed and manufactured, tested and analysis by FEA have been done. Static torsion test was carried out for a hybrid aluminum glass fiber composite drive shaft. Hybrid shaft having stacking sequence $[\pm 45]_s$ with different number of layers were studied. The conclusions obtained in this experimental study are summarized as follow:

1. Failure modes of both torsion were studied
2. Fiber orientation and number of layers strongly affect the static torsion capacity of a hybrid aluminum/composite drive shaft.
3. The torque capacity is increased for Hybrid shaft $[\pm 45]_s$ laminates, approximately 66% higher than the pure aluminum tube
4. Increasing the number of composite layers would increase the fatigue strength for a hybrid aluminum/composite drive shaft;

The conclusions obtained in FEA analysis of full scale hybrid shaft are summarized as follow:

1. The Design Von Mises Stress obtained for hybrid drive shaft is 6 times the allowable stress
2. Shear stress obtained for hybrid shaft is 37% higher than steel drive shaft
3. Total deformation of the hybrid shaft is 60% less than steel drive shaft.
4. The highest bending natural frequency obtained for Hybrid shaft is 293.613 Hz (17616.78 rpm) which is 63 % higher than required bending natural frequency 108 Hz(6500rpm)

REFERENCES

1. Lee, D.G., Kim, H.S., Kim, J.W., and Kim, J.K. 2004. Design and manufacture of an automotive hybrid aluminum/composite drive shaft.
2. Kim H. S. and Lee, D. G. (2005), Optimal design of the press fit joint for a hybrid aluminum/composite drive shaft, Composite Structure, in press.
3. Jin Kook Kim, Dai Gil Lee, and Durk Hyun Cho, 2001, "Investigation of Adhesively Bonded Joints for Composite Propeller shafts", Journal of Composite Materials, Vol.35, No.11, pp.999-1021.
4. Cho D. H. and Lee D. G. (1997), Manufacturing of co-curing aluminum composite shafts with compression during co-curing

5. Shokrieh M. M, Hasani K. and Lessard L. B. (2004), Shear buckling of a composite drive shaft under torsion, Composite Structure, 64: 63-69.
6. Bang, K. G. and Lee, D. G. (2000), Design of carbon fiber composite shaft for high-speed air spindles, Composite Structures, 55: 247-259
7. Kim, J. K, Lee, D. G., and Cho D. H., (2001), Investigation of Adhesively Bonded Joints for Composite Propeller Shafts. J. Composite material, 35: 999-1019.
8. Rangaswamy, T & Vijayarangan, S. & Chandrashekar, R.A. & Venkatesh, T.K. & Anantharaman, K. (2002) "Optimal design and analysis of automotive composite drive shaft", International Symposium of Research Students on Materials Science and Engineering, 2004, 19.
9. Lee, D. G., Kim J. W. and Hwang H. Y., (2004). Torsional fatigue characteristics of Aluminum/Composite co-cured shafts with axial compressive preload, J. of Composite Materials, 38:737-756.
10. PSGCT, Design Data. India.1995
11. Timoshenko, S. P., Gere, J. M. Theory of Elastic Stability. McGraw-Hill, NY, 1963:pp. 500 – 509.
12. Rao, S. S. Mechanical Vibrations. Addison-Wesely Publishing Company, NY: pp. 537 – 541.
13. Cho DH, Lee DG, Choi JH. Manufacturing of one-piece automotive drive shafts with aluminum and composite materials. Compos Struct 1997;38:309-19.
14. Lalanne M, Berthier O, Hagopian JD, Nelson FC. Mechanical Vibration for Engineers. New York: John Wiley and Sons; 1983. p. 102-5.
15. Gibson RF. Principles of the Composite Material Mechanics. New York: McGraw-Hill; 1994. p. 110-2.
16. Mallick PK. Fiber-Reinforced Composites. New York: Marcel Dekker; 1988. p. 2-3.



M. Arun, Scholar of M.E. Product Design and commerce, Department of Production Engineering, PSG College of Technology, Coimbatore, India.



K. Somasundara Vinoth, Assistant Professor and Research Scholar, Department of Production Engineering, PSG College of Technology, Coimbatore, India.